Preprints of the 21st IFAC World Congress (Virtual)
Berlin, Germany, July 12-17, 2020

Optimal Estimation and Feedforward Control of Strip-Longitudinal Hardness for Thickness Hunting Suppression of Tandem Cold Mill Process ⋆

Hoyong Lee * **Seungmin Hur** ** **Kyungsik Woo** **
Dongjun Lee *

* *Department of Mechanical & Aerospace Engineering and IAMD, Seoul National University, Seoul, Korea (e-mail: {hylee0428, djlee}@snu.ac.kr).*
** *Hyundai Steel Company R & D Center, Chungcheongnam-do, Korea (e-mail: {wooks, smhur}@hyundai-steel.com)*

Abstract: Following the recent trend of weight reduction in car industry, producing high quality cold-rolled AHSS (advanced high-strength steel) strip becomes important. Thickness hunting (or fluctuation) problem can be more prominent for this cold-rolled AHSS strip making, which can stem from the non-uniformity of hot-rolled strip and can severely degrade product quality. In this paper, we propose a novel framework to estimate the strip-longitudinal hardness of the TCM (tandem cold mill) process and its feedforward control to substantially reduce the thickness hunting, while fully incorporating the interconnected nature and sensing sparsity of the TCM process. In particular, our estimator consists of the following two complementary loops: 1) fast real-time hardness estimation loop, which optimally fuses the process model and sensing information; and 2) slower constant process-parameter estimation loop via optimization utilizing the nonlinear process model and (stored/measured) sensor data. Efficacy of the proposed estimation and control frameworks are then validated with high-precision TCM process physics simulator.

Keywords: Feedforward control, process parameter estimation, sensor fusion, steel manufacturing process, unscented transformation

1. INTRODUCTION

Cold-rolled steel strip, which is made from hot-rolled steel strip through TCM (tandem cold mill) process, is used for automobiles, appliances, construction materials, etc., due to its thin thickness and elegant surface. Recently, following the trend of weight reduction in car industry, demand for cold-rolled AHSS (advanced high-strength steel) strip has increased and it becomes important to produce high quality cold-rolled AHSS strip. For certain kind of cold-rolled AHSS strip, however, thickness hunting (or fluctuation) larger than product quality criteria can easily occur. The main source of this thickness hunting is known to be the non-uniform hardness of hot-rolled steel strip (Choi et al. (1994)) fed to the TCM process. Here, the notation hardness comprehensively means metallurgical characteristic affecting deformation resistance of the strip.

Suppression of this thickness hunting is challenging, since, in typical industrial TCM settings, sensors directly and real-time measuring this non-uniform hardness of the steel strip and also affordable enough for real deployment simply do not exist. This hardness estimation challenge is even further exacerbated with the scarcity/sparsity of sensors and the interconnected nature of the TCM process with inter-stands transport delay - see Fig. 1.

In this paper, we propose a novel estimation framework for this hardness of the steel strip in the TCM process. For this, we assume that the hardness (and other metallurgical property) non-uniformity is mostly along the strip-longitudinal direction (i.e., direction passing through TCM rolls) and construct the TCM process model with this longitudinal hardness variation. Based on this process model, we then derive our hardness estimator, which consists of the following two complementary loops: 1) fast updating loop for hardness estimation in the manner of sensor fusion, by optimally fusing the process model and the sensor information with their respective uncertainties also taken into account; and 2) slowly updating loop for constant process-parameter estimation in the manner of nonlinear optimization, by exploiting the high-rate data stream received/stored from available sensors and the nonlinear TCM process model.

More specifically, the hardness estimation loop is: 1) running fast (e.g., 0.02sec. in Sec. 4) so that the estimated (longitudinal) hardness can be used for high-rate control for better hunting suppression performance; 2) utilizing UT (unscented transformation (Julier (2002); Ha et al. (2018))) to more precisely propagate random vari-

⋆ Research supported in part by Hyundai Steel Company 0420-20180046.

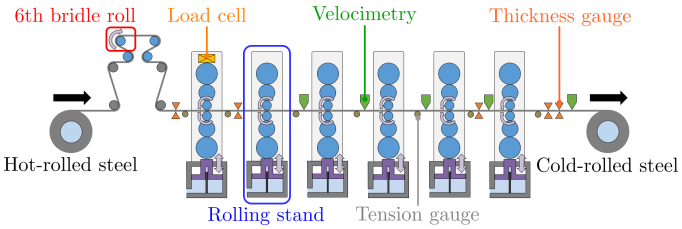

Fig. 1. Tandem cold mill (TCM) process diagram with six rolling stands, five of which are involved in thickness control, and one bridle roll.

ables through the nonlinear TCM process model (than, e.g., EKF (extended Kalman filtering (Jazwinski (2007))) scheme), which can then be optimally fused with sensor measurements (with sensor uncertainties typically given by their manufacturers); and 3) fully respecting the sensor scarcity and interconnected nature of the TCM process, using only available sensors at each roll and gradually improving the sensing accuracy across each roll through the TCM process as more information is collected and optimally exploited down to the last roll. On the other hand, the constant parameter estimation loop is: 1) running slow (e.g., 5sec. in Sec. 4), which is enough since the process parameters to estimate here can be assumed constant; 2) taking advantage of large amount of TCM process data, which is collected and stored from high-rate data stream of measuring instruments during the TCM operation; and 3) trying to find the best estimate of the constant process-parameters via nonlinear optimization based on the (complex/nonlinear) TCM process model.

We also propose a feedforward control framework, which, by utilizing this real-time estimated longitudinal hardness information, can substantially reduce the thickness hunting although its synthesis and structure are rather simple. These proposed hardness estimation and feedforward control frameworks are then all validated with high-precision TCM process physics simulator running based on real TCM process data.

Some on-line estimation schemes of the strip-longitudinal hardness (or deformation resistance) have been proposed for the rolling mill process (e.g., Wang et al. (2005); Bu et al. (2019); Prinz et al. (2019)), which, however, are based on the batch optimization technique for one single roll stand, thus, not able to properly take into account neither the modeling and sensing uncertainties (and the optimality of their fusion) nor the interconnected structure of the TCM process. On the other hand, some control results have also been proposed, where the hardness (and other parameter) variations are lump-modeled as disturbance and H∞ control or state-dependent LQR (linear quadratic regulator) are applied to suppress this disturbance effect (e.g., Geddes and Postlethwaite (1998); Pittner and Simaan (2006, 2008)). Although effective in reducing the thickness hunting, these control results, however, do not provide the longitudinal hardness information, which, by itself, can be very useful for other purposes in industrial setting (e.g., strip quality sensing) or can be flexibly used for other control techniques (e.g., model predictive control). To our knowledge, our estimation framework presented in this paper is the very first result, which optimally fuses process model and multi-sensor information while fully incorporating their uncertainties and the interconnected structure of the TCM process.

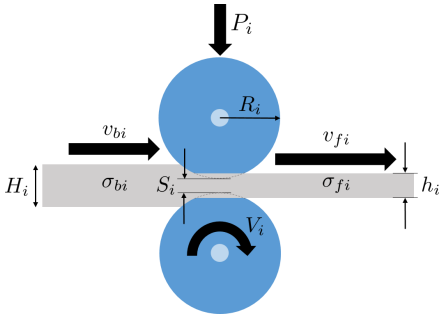

Fig. 2. Rolling between two work rolls of the ith stand

The rest of the paper is organized as follows. The nonlinear modeling of the TCM process, which is used both for our estimation and control frameworks, is presented in Sec. 2. The main result - optimal hardness estimation framework - is then derived in Sec. 3, and the feedforward control design and validation results with high-precision physics-based TCM simulator explained in Sec. 4. Sec. 5 concludes the paper with summary.

2. MODELING OF TCM PROCESS

Tandem cold mill (TCM), which produces cold-rolled steel strip from hot-rolled steel strip, is composed of bridle rolls, rolling stands, and various measuring instruments (e.g., loadcell, thickness gauge, tension gauge, and velocimetry) as shown in Fig. 1 where the bridle roll feeds hot-rolled steel strip in TCM, and rolling stand deforms the strip and transports it to the next stand. About the rolling stand, for example, strip of thickness H_i entering rolling stand with speed v_{bi} and tension stress σ_{bi} is deformed by the stand of roll gap S_i and roll speed V_i under force P_i and then becomes strip of thickness h_i with speed v_{fi} and tension stress σ_{fi} as shown in Fig. 2. The exact notations about rolling through the ith stand is specified in table 1.

Table 1. Notations for the ith rolling stand

Notation	Physical meaning
P_i	Rolling force given to ith stand
H_i	Entry thickness of ith stand
h_i	Exit thickness of ith stand
σ_{bi}	Back tension stress between $(i-1)$th and ith stand
σ_{fi}	Front tension stress between ith and $(i+1)$th stand
v_{bi}	Entry strip speed of ith stand
v_{fi}	Exit strip speed of ith stand
S_i	Roll gap between undeformed work rolls of ith stand
V_i	Roll (linear) speed of ith stand
R_i	Work roll radius of ith stand

Rolling, which is plastic and nonlinear deformation of the strip between two work rolls, has been studied for several decades (e.g., Orowan (1943), Bland and Ford (1943), Bland et al. (1952), Bryant (1973)). Among the existing models, we choose Bland-Ford-Hill model for our TCM model due to its closed-form equations, which can be represented as

$$P_i = W(\bar{k}_i - \bar{\sigma}_i)\sqrt{R'_i(H_i - h_i)}D_{pi}$$
$$f_i = \tan^2\left(\frac{1}{2}\sin^{-1}\sqrt{r_i} + \frac{1}{4\mu_i}\sqrt{\frac{h_i}{R'_i}}\ln\left(\frac{h_i}{H_i}\frac{1-\sigma_{bi}/k_{bi}}{1-\sigma_{fi}/k_{fi}}\right)\right) \tag{1}$$

where f_i is forward slip, which relates roll speed and exit strip speed as

$$v_{fi} = (1 + f_i)V_i, \tag{2}$$

and W is width of steel, and k_{bi}, k_{fi}, $\bar{k}_i$ are deformation resistances, each of which means value at stand entrance, value at stand exit, and mean value across the roll-bite region, respectively. These deformation resistances can be expressed as modeled in (Roberts (1978)).

$$\begin{aligned}\bar{k}_i &= 1.155(\alpha(\bar{r}_i + \beta)^\gamma + a\log_{10}(1000\dot{\varepsilon}_i))\\ k_{bi} &= 1.155(\alpha(r_{bi} + \beta)^\gamma + a\log_{10}(1000\dot{\varepsilon}_i))\\ k_{fi} &= 1.155(\alpha(r_{fi} + \beta)^\gamma + a\log_{10}(1000\dot{\varepsilon}_i))\end{aligned} \tag{3}$$

where α, β, γ, a are metallurgical parameters of steel, and r_{bi}, r_{fi}, $\bar{r}_i$ are thickness reduction ratios of strip given as

$$\begin{aligned}\bar{r}_i &= 0.4r_{bi} + 0.6r_{fi}\\ r_{bi} &= 1 - H_i/H_a\\ r_{fi} &= 1 - H_i/H_a\end{aligned} \tag{4}$$

Here, H_a is annealed thickness of hot-rolled steel, which can be considered as initial thickness of strip before it enters TCM. Also note that entry thickness of the first stand H_1 is same as the annealed thickness. The variable ε_i is local strain at exit of the ith stand and its derivative is given as

$$\dot{\varepsilon}_i = 0.0358V_i\sqrt{\frac{r_i}{2R_iH_i}} \tag{5}$$

Also note that $r_i = 1 - h_i/H_i$ of equation (5) is local thickness reduction ratio for each rolling stand, and aforementioned r_{bi}, r_{fi}, $\bar{r}_i$ are reduction ratios respect to annealed thickness of hot-rolled steel.

Going back to equation (1), $\bar{\sigma}_i$, R'_i, and D_{pi} are mean tension stress, deformed work roll radius, and approximate value of $f_3(a, r)$ specified in (Bland and Ford (1943)), respectively and given as

$$\begin{aligned}\bar{\sigma}_i &= \frac{2}{3}\sigma_{bi} + \frac{1}{3}\sigma_{fi}\\ R'_i &= R_i\left(1 + \frac{16(1-\nu_R^2)}{\pi W E_R(H_i - h_i)}P_i\right)\\ D_{pi} &= 1.08 - 1.02r_i + 1.79\mu_i r_i\sqrt{\frac{R'_i}{H_i}}\end{aligned} \tag{6}$$

where ν_R and E_R are Poisson's ratio and Young's modulus of work roll, respectively, and μ_i is friction coefficient between work roll and strip, which is given as

$$\mu_i = \sqrt{\frac{H_i - h_i}{2R_i}}\left(0.5 + (K_{i1} - 0.5)e^{-K_{i2}V_i}\right) \tag{7}$$

with constants K_{i1} and K_{i2}.

Apart from the theoretic rolling model, we also have a simple empirical relation between roll gap and exit thickness as

$$h_i = S_i + \frac{P_i}{K_i} \tag{8}$$

where K_i is mill stretch constant, which can be considered as spring coefficient of rolling stand, for the ith stand. Also, with the assumption that strip only deforms along strip-longitudinal direction (i.e., direction of strip transporting), mass flow conservation at the ith rolling stand can be simply expressed as

$$H_i v_{bi} = h_i v_{fi} \tag{9}$$

Therefore, physical phenomenon under rolling stand is expressed by equations (1), (8), and (9) where equations (2) to (7) are included in equation (1) and the subscript i shown in equations (1) to (9) means the corresponding variable or constant of the ith rolling stand. Note that effect of parameters such as surface roughness and temperature are neglected because this paper focuses on addressing thickness hunting stem from the non-uniform hardness.

The TCM model can be constructed by connecting multiple rolling stands serially. Then we can find relation between two adjacent stands. First, with the assumption that tension stress is homogeneous in strip between two adjacent stands (i.e., fast enough tension stress dynamics), front and back tension stresses can be related as

$$\sigma_{fi} = \sigma_{b(i+1)} \tag{10}$$

Secondly, from the well known stress-strain relationship $\sigma = E\varepsilon$ and its differential form, tension stress dynamics, which relates derivative of front tension stress and strip speed terms, is obtained as

$$\dot{\sigma}_{fi} = \frac{E}{L_i}(v_{b(i+1)} - v_{fi}) \tag{11}$$

where E and L_i are Young's modulus of steel and distance between the ith and $(i+1)$th rolling stand, respectively. Note that equations (10) and (11) physically connect the adjacent stands.

From transportation characteristic of TCM, which means certain part of strip passing through the ith rolling stand will arrive the $(i+1)$th stand after certain delay (e.g., from about 0.9 second to 5 seconds for our case), and the assumption that thickness is preserved while transporting, entry and exit thicknesses are related as

$$H_{i+1}(t) = h_i(t - \tau_{i,i+1}(t)) \tag{12}$$

where $\tau_{i,i+1}(t)$ is transport delay between the ith and $(i+1)$th rolling stand satisfying

$$L_i = \int_{t-\tau_{i,i+1}}^{t} v_{fi}(t)dt \tag{13}$$

In other words, certain part of strip that reaches the $(i+1)$th rolling stand at time t departed from the ith stand $\tau_{i,i+1}(t)$ ago.

In order to utilize this transportation characteristic of TCM process while considering hardness non-uniformity of hot-rolled steel strip, we assume that the metallurgical property including hardness non-uniformity is mostly along the strip-longitudinal direction. Then hot-rolled steel strip can be modeled as group of numerous strip-longitudinal segments, each of which has its own metallurgical parameters as shown in Fig. 3. Metallurgical parameters of the sth segment are given as $H_a(s)$, $\alpha(s)$, $\beta(s)$, $\gamma(s)$, and $a(s)$, domain of which are longitudinal dimension. Here, based on experimental results, we assume that $\alpha(s)$, which is directly proportional to resistance deformation of equation (3), is dominant parameter corresponding to non-uniform hardness of hot-rolled steel strip. Therefore,

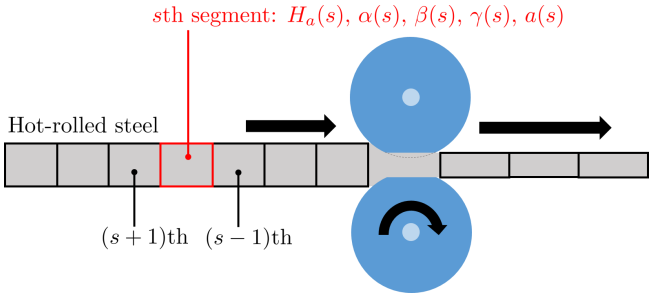

Fig. 3. Hot-rolled steel strip is assumed to be composed of numerous strip-longitudinal segments, each of which has its own metallurgical parameters.

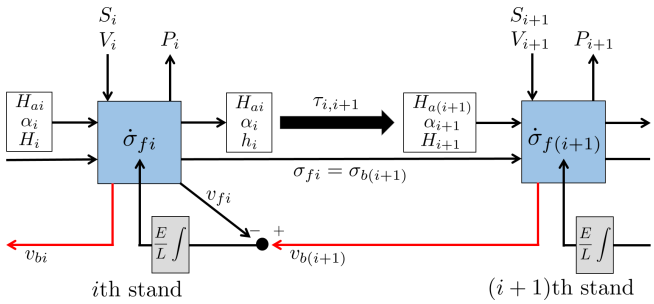

Fig. 4. Structure of TCM model constructed by connecting rolling stands serially while incorporating interplay between adjacent stands.

we define $\alpha(s)$ as representative hardness parameter and β, γ, and a as metallurgical constants. We can also view longitudinally varying metallurgical parameters $H_a(s)$ and $\alpha(s)$ from the ith stand by defining $H_{ai}(t)$ and $\alpha_i(t)$, meaning of which are $H_a(s)$ and $\alpha(s)$ when the sth segment arrives the ith stand at time t, respectively. Then we can easily find that these $H_{ai}(t)$ and $\alpha_i(t)$ also have transportation relation with same transport delay of equation (12) as

$$\begin{aligned} \alpha_{i+1}(t) &= \alpha_i(t - \tau_{i,i+1}(t)) \\ H_{a(i+1)}(t) &= H_{ai}(t - \tau_{i,i+1}(t)) \end{aligned} \tag{14}$$

Note that α of equation (3) and H_a of equation (4) should be changed to α_i and H_{ai} from now on, respectively, to incorporate our assumption of strip-longitudinal metallurgical parameters to TCM process model. Also note that representative hardness parameter satisfying the transportation characteristic can be utilized for more accurate estimation, which is detailed in Sec. 3.

Finally, using the physical connection between adjacent stands (i.e., equations (10) and (11)) and the transportation relation (i.e., equations (12) and (14)), TCM process model considering non-uniform hardness is established as shown in Fig. 4 by connecting rolling stands serially. Note that structure of the established model is similar to cascaded model but not because the entry strip speed (i.e., red flow in Fig. 4), affects the tension dynamics of former adjacent stand, which makes the nonlinear TCM process model even more complex.

3. OPTIMAL HARDNESS ESTIMATOR DESIGN

From the established TCM process model considering non-uniform hardness of hot-rolled steel strip and its inter-stands transportation, we design a novel framework to estimate the strip-longitudinal hardness information to address the thickness hunting (or fluctuation) problem occurred in cold-rolled AHSS strip. Remark that proposed estimation framework can be considered as virtual sensor for hardness, which virtually measures hardly observable metallurgical property on-line by exploiting information of existing sensors and the TCM process model.

Besides the hardness, there are also indirectly measurable or unmeasurable TCM process data due to restriction of sensor deployment and sensing sparsity of TCM. Considering our TCM shown in the Fig. 1, for example, entry and exit thicknesses are indirectly measurable by using transportation characteristic because thickness gauges have distance from rolling stand or even absent. Similarly, exit strip speed for the first stand is also indirectly measurable due to the absent of velocimetry at exit side of the stand. Metallurgical parameters and friction constants of equation (7) even do not have corresponding measuring instruments. Therefore, estimation objectives for our system is as summarized in table 2 where α_i, H_{ai}, H_i, h_i, v_{f1} are defined as estimation variables and β, γ, a, K_{i1}, K_{i2} as unknown (constant) process-parameters.

Table 2. Estimation objectives

	Notations
Estimation variables	α_i, H_{ai}, H_i, h_i, v_{f1}
Unknown process-parameters	β, γ, a, K_{i1}, K_{i2}

Sensor measurement of TCM is directly provided by measuring instruments (i.e., load cell, thickness gauge, tension gauge, and velocimetry) and inherent sensors of rolling stands (i.e., pressure gauge, motor encoder, and potentiometer). These multi-sensor information and known (constant) process-parameters (e.g., width and Young's modulus of hot-rolled steel, metallurgical specification and radius of work rolls, mill stretch constants, and distances between adjacent stands), which is obtained prior to the process, for our TCM system are specified in table 3 where X means thickness gauge measurement and subscripts E and D correspond to entry and exit side of stand, respectively.

Table 3. Multi-sensor information and known process-parameters of TCM process

	Notations
Multi-sensor information	P_i, σ_{bi}, σ_{fi}, v_{b1}, $v_{fi(i\neq 1)}$, S_i, V_i, $X_{1\mathrm{E}}$, $X_{1\mathrm{D}}$, $X_{5\mathrm{D}}$
Known process-parameters	W, E, E_R, ν_R, L_i, R_i, K_i

In order to optimally fuse the process model and the sensor information with their respective uncertainties also taken into account, sensor measurements are considered as normal random variables where this assumption is typical for treating sensors. Then, mean and variance of all the sensor information notated in table 3 is obtained from measurements during TCM process and error specifications provided by sensor manufacturers, respectively. For example, back tension stress is given with its normal distribution as

$$\sigma_{bi,k} \sim \mathcal{N}(\mu_{\sigma_{bi},k}, Q_{\sigma_{bi},k})$$

where $\mu_{\sigma_{bi},k}$ is back tension stress from tension gauge, $Q_{\sigma_{bi},k}$ is variance of the back tension stress from sensor

specification, and k indicates corresponding variables of kth time step in discrete time domain. Note that the variances of sensor information are assumed to be constant (i.e., $Q_{\sigma_{bi},k} = Q_{\sigma_{bi}}$).

Then, the known distributions of multi-sensor information can be propagated through the process model (i.e., fusing of sensor measurement and the process model), which lead us to find normal distributions of estimation variables in table 2. Normal distribution of h_i, for instance, is obtained by propagating distributions of sensor information S_i and P_i through equation (8) as

$$\begin{aligned} \mu_{h_i,k} &= \mu_{S_i,k} + \mu_{P_i,k}/K_i \\ Q_{h_i,k} &= Q_{S_i} + Q_{P_i}/K_i^2 \end{aligned} \tag{15}$$

where $\mu_{\star,k}$ and $Q_{\star,k}$ indicate mean and variance of variable $\star$ at kth time step, respectively. Note that Q_{S_i} and Q_{P_i} are constants and therefore $Q_{h_i,k}$ is also constant.

Similar to equation (12), relation between thickness gauge measurement and entry thickness is given as

$$H_i(t) = X_{i\mathrm{E}}(t - \tau_{i\mathrm{E}}(t)) \tag{16}$$

with the transport delay $\tau_{i\mathrm{E}}(t)$ satisfying

$$L_{i\mathrm{E}} = \int_{t-\tau_{i\mathrm{E}}}^{t} v_{bi}(t)dt \tag{17}$$

where $L_{i\mathrm{E}}$ is distance between the ith stand and thickness gauge at entry side of the ith stand. In other words, a strip segment that reaches the ith stand at time t departed from the entry thickness gauge of the ith stand $\tau_{i\mathrm{E}}(t)$ ago. Note that our estimation framework uses $\tau_{i\mathrm{E}}(t) = L_{i\mathrm{E}}/v_{bi}(t)$ and $\tau_{i,i+1}(t) = L_i/v_{fi}(t)$ as transport delays for simplicity while accurate hardness estimation is still possible - see Sec. 4. Then, normal distribution of H_i is gained by propagating the distribution of $X_{i\mathrm{E}}$ through equation (16) as

$$\begin{aligned} \mu_{H_i,k} &= \mu_{X_{i\mathrm{E}},k-k_{i\mathrm{E}}} \\ Q_{H_i,k} &= Q_{X_{i\mathrm{E}}} \end{aligned} \tag{18}$$

where $k_{i\mathrm{E}}$ is discrete time step corresponding to transport delay $\tau_{i\mathrm{E}}(t)$. Similarly, propagating through equation (12), another normal distribution of H_i is procured as

$$\begin{aligned} \mu_{H_i,k} &= \mu_{h_{i-1},k-k_i} \\ Q_{H_i,k} &= Q_{h_{i-1},k-k_i} \end{aligned} \tag{19}$$

where k_i is discrete time step corresponding to transport delay $\tau_{i-1,i}(t)$. In the same way, normal distributions for α_i and H_{ai} are obtained through the transportation relation of equation (14) as

$$\begin{aligned} \mu_{\alpha_i,k} &= \mu_{\alpha_{i-1},k-k_i} \\ Q_{\alpha_i,k} &= Q_{\alpha_{i-1},k-k_i} \\ \mu_{H_{ai},k} &= \mu_{H_{a(i-1)},k-k_i} \\ Q_{H_{ai},k} &= Q_{H_{a(i-1)}} \end{aligned} \tag{20}$$

Considering material continuity, which assumes strip-longitudinal metallurgical parameters of adjacent strip segments are almost identical, representative hardness parameter can be modeled as random-walk process with white Gaussian noise w_α as

$$\alpha_i(t) = \alpha_{i-1}(t) + w_\alpha \tag{21}$$

Then normal distribution from equation (21) is given as

$$\begin{aligned} \mu_{\alpha_i,k} &= \mu_{\alpha_i,k-1} \\ Q_{\alpha_i,k} &= Q_{w_\alpha} \end{aligned} \tag{22}$$

where Q_{w_α} is variance of w_α. Note that this continuity information is inserted to our estimation framework to induce physically reasonable hardness estimation.

The mass flow conservation of equation (9) can be expressed as

$$v_{fi} = g(H_i, v_{bi}, h_i), \quad h_i = g(H_i, v_{bi}, v_{fi}) \tag{23}$$

where the left equation for v_{fi} corresponds to $i = 1$ and the right equation for h_i corresponds to $i = 2, \cdots, 5$ for our TCM and g is a nonlinear map defined as

$$g(\chi_1, \chi_2, \chi_3) \equiv \frac{\chi_1 \chi_2}{\chi_3} \tag{24}$$

Then, normal distributions of v_{fi} (or h_i) is obtained by propagating known distributions of H_i, v_{bi}, and h_i (or v_{fi}) via nonlinear map g . In order to propagate distributions through the nonlinear map, unscented transformation (UT) is adopted, s.t.,

$$\begin{aligned} v_{fi,k} &= \mathrm{UT}_{g,\,(H_{i,k}, v_{bi,k}, h_{i,k})} \approx \mathcal{N}(\mu^{\mathrm{UT}}_{v_{fi},k}, Q^{\mathrm{UT}}_{v_{fi},k}) \\ h_{i,k} &= \mathrm{UT}_{g,\,(H_{i,k}, v_{bi,k}, v_{fi,k})} \approx \mathcal{N}(\mu^{\mathrm{UT}}_{h_i,k}, Q^{\mathrm{UT}}_{h_i,k}) \end{aligned} \tag{25}$$

where $\mathrm{UT}_{g,\star}$ is the unscented transformation through the nonlinear map $g(\star)$. Similarly, from equation (1), representative hardness parameter is given as

$$\begin{aligned} \alpha_i &= (\bar{r}_i + \beta)^{-\gamma}(0.8658\bar{k}_i - a\log_{10}(1000\dot{\varepsilon}_i)) \\ &\equiv g_\alpha(H_{ai},\, H_i,\, h_i,\, P_i,\, V_i,\, \sigma_{bi},\, \sigma_{fi}) \end{aligned} \tag{26}$$

with nonlinear map g_α of variables with known distributions. Then normal distribution of $\alpha_{i,k}$ is obtained by utilizing UT as

$$\alpha_{i,k} = \mathrm{UT}_{g_\alpha,\,(H_{ai}, H_i, h_i, P_i, V_i, \sigma_{bi}, \sigma_{fi})} \approx \mathcal{N}(\mu^{\mathrm{UT}}_{\alpha_i,k},\, Q^{\mathrm{UT}}_{\alpha_i,k}) \tag{27}$$

Note that unknown process-parameters of table 2 is used for equation (27), which leads us to development of another estimation loop for the unknown (constant) process-parameters detailed later in this section.

Among the procured normal distributions, redundant information exist for certain variables (e.g., H_i, h_i, and α_i). For example, distributions of H_i for $i = 2$ is observed from the both equations (18) and (19). By using well known optimal fusion of two normal distributions (Winkler (1981)), redundant information can be combined to more accurate (i.e., smaller variance) normal distribution, which is in a manner of sensor fusion. Then, normal distribution of H_2 from the sensor fusion is gained as

$$H_{i,k} \sim \mathcal{N}(\mu^{\mathrm{SF}}_{H_i,k}, Q^{\mathrm{SF}}_{H_i}) \tag{28}$$

where the mean and variance are simply calculated from the distributions before merging. Note that propagating optimally fused distribution of H_2 through the process model (e.g., equation (23) and (26) also leads to more believable information of h_2. In the same way, from the equation (15) and (25) with fused distribution of H_2, optimally fused normal distribution of h_i can be obtained for $i = 2, \cdots, 5$.

$$h_{i,k} \sim \mathcal{N}(\mu^{\mathrm{SF}}_{h_i,k}, Q^{\mathrm{SF}}_{h_i}) \tag{29}$$

Similarly, distribution for $\alpha_{i,k}$ in a manner of sensor fusion is gained from equation (20), (22), and (27) with the other optimally fused information.

$$\alpha_{i,k} \sim \mathcal{N}(\mu^{\mathrm{SF}}_{\alpha_i,k}, Q^{\mathrm{SF}}_{\alpha_i,k}) \tag{30}$$

In this case, for instance, to fully exploit the advantage of information fusion, distributions of equation (22) and (27) are firstly merged for $i = 1$. Then, utilizing the optimally

fused information of α_1, distribution of α_2 is obtained from the equation (20), (22), and (27). Again, optimally fused information of α_2 is used for merging of α_3 distributions from the same three equations and same as other stands (i.e., $i = 4, 5$).

Therefore, normal distributions for all the estimation variables, including representative hardness parameter, are procured by optimally fusing multi-sensor information and the process model while UT is adopted to more precisely propagate random variables through the nonlinear process model. Note that this estimation based on sensor fusion fully respects the sensor scarcity and interconnected nature of the TCM process by using only available sensors at each stand. Also note that all the calculation along estimation is explicit, which leads to fast update rate of the estimation loop.

However, unknown process-parameters in table 2 are assumed to be known and used to get the result of equation (27). Therefore, another estimation for the constant process-parameters is needed. Thanks to large amount of TCM process data, stored/measured process data (of current strip) can be utilized to estimation the process-parameters by solving nonlinear optimization. With the assumption that estimation variables of table 2 are given from the aforementioned estimation loop of sensor fusion, nonlinear optimization, goal of which is to find unknown process-parameters that satisfy the Bland-Ford-Hill rolling model of equation (1), is constructed as

$$\xi = \arg\min \sum_{i=1}^{N_s} \sum_{j=1}^{N_d} \left(\left(1 - \frac{\hat{P}_i(\xi, j)}{P_i(j)} \right)^2 + \left(1 - \frac{\hat{v}_{fi}(\xi, j)}{v_{fi}(j)} \right)^2 \right) \tag{31}$$

where $\xi \equiv [\beta, \gamma, a, K_{i1}, K_{i2}]$ is composed of unknown process-parameters, and N_s and N_d are number of stands (e.g., 5 for our TCM) and time steps for process data accumulation (e.g., 2500 for our case), respectively. Here, $P_i(j)$ and $v_{fi}(j)$ are measurement of rolling force and exit strip speed, respectively, and $\hat{P}_i(\xi, j)$ and $\hat{v}_{fi}(\xi, j)$ are calculated ones from current ξ and estimated variables via equation (1). This estimation loop for constant process-parameters needs time to store the process data and solve the nonlinear optimization, which leads to slow update rate compare to the estimation loop based on sensor fusion.

In summary, our optimal hardness estimator is developed in two complementary estimation loops, one of which optimally fuses multi-sensor information and the nonlinear/complex TCM process model in a manner of sensor fusion to obtain normal distributions of estimation variables including hardness, and the other utilizes rich TCM process data to estimate unknown process-parameters by solving nonlinear optimization. Structure of the proposed estimation framework with two complementary loops is shown in the Fig. 5.

4. FEEDFORWARD CONTROL DESIGN AND VALIDATION

In order to validate the efficacy of proposed hardness optimal estimator, in-house TCM simulator developed and validated in the funding company, is used. This high-precision physics-based TCM simulator behaves similar to

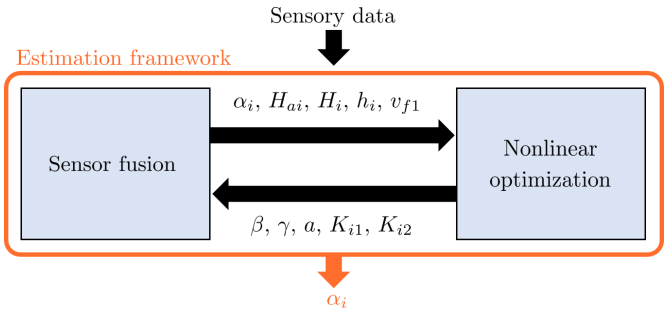

Fig. 5. Structure of proposed optimal hardness estimator

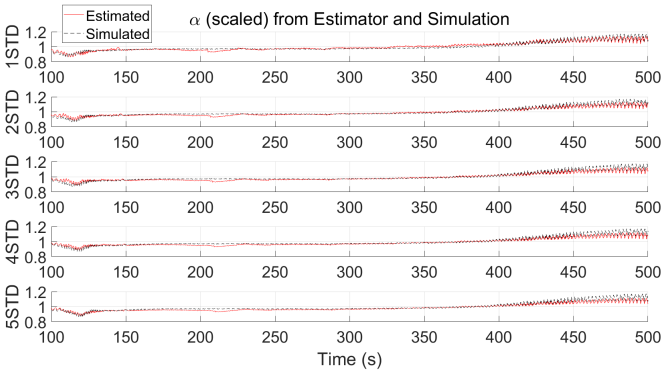

Fig. 6. Representative hardness parameter α_i from the estimator and simulation result

the actual TCM process, with its parameters, including the representative hardness parameter $\alpha(s)$, extracted from the actual TCM process data. The estimation loop based on sensor fusion (or nonlinear optimization) of the proposed estimator update the results by every 0.02sec. (or 5sec.) for our TCM simulator. Performing the TCM simulation with our proposed hardness optimal estimator, representative hardness parameter α_i from the estimator (i.e., blue lines) and simulation result (i.e., black dashed lines) are given as in Fig. 6 where the simulation result is treated as ground truth. The RMSE data is The RMSE (root mean square error) of the estimated representative hardness parameter α_i for each stand is given as table 4, which shows accurate estimation performance of the proposed hardness estimator. The normalized error is used for calculating RMSE due to data security.

Table 4. RMSE of the estimation for α_i

Stand number	1	2	3	4	5
RMSE (%)	2.09	1.99	1.95	1.90	1.92

Note that the estimation error has tendency of decreasing by passing through TCM process, which can be explained by variances of α_i from the estimator - see Fig. 7. For example, as detailed in Sec.3, α_1 is estimated by optimally fusing sensor information and the process model correspond to the 1st stand. Then α_2 estimation is performed by optimally merging sensor measurement, the process model for the 2nd stand, and additionally transported optimally fused α_1 information, which leads smaller variance (i.e. more accurate estimation) by exploiting information of the both 1st and 2nd stand. In the same way, therefore, ith stand can take advantage of exploiting information

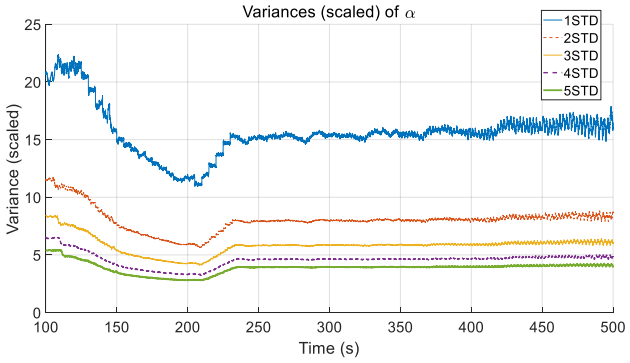

Fig. 7. Variances of α_i from proposed hardness estimator

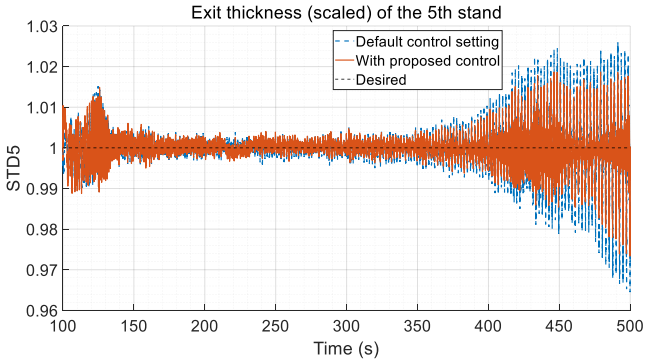

Fig. 8. TCM simulation result for exit thickness of 5th stand for default control structure and our proposed controller

obtained from 1st stand to ith stand and most accurate hardness estimation is achieved for the last stand of the TCM process.

In order to utilize our real-time optimal hardness estimator for thickness hunting suppression, we design a feedforward controller that uses estimated representative hardness parameter transported from the former stand as feedforward to control exit thickness. In order to respect the existing industrial control structure of TCM composed of numerous single objective controllers, and to reduce the risk for adjustment to real system, a retrofit controller, which can be equipped to existing control structure, is considered. Then, not only following concept of existing TCM feedforward controller, which uses transported entry thickness as feedforward, but also considering longitudinally varying hardness, partial differential form respect to entry thickness and representative hardness parameter for equation (8) is considered.

$$\Delta S = \frac{\partial h}{\partial H}\Delta H + \frac{\partial h}{\partial \alpha}\Delta\alpha - \frac{1}{K}\left(\left.\frac{\partial P}{\partial H}\right|_{*} \Delta H + \left.\frac{\partial P}{\partial \alpha}\right|_{*} \Delta\alpha \right) \tag{32}$$

where Δ indicates difference from the nominal state and $*$ indicates derivative value at nominal state. Therefore, to maintain exit thickness from varying entry thickness and hardness, ΔS, which is control input for rolling stand, should be given as

$$\Delta S = -\frac{1}{K}\left(\left.\frac{\partial P}{\partial H}\right|_{*} \Delta H + \left.\frac{\partial P}{\partial \alpha}\right|_{*} \Delta\alpha \right) \tag{33}$$

The nominal partial derivative values can be calculated by differentiating rolling force equation (1). Note that this simple structure retrofit controller can replace existing feedback controller while maintaining the other controllers.

In order to validate the efficacy of proposed feedforward controller for thickness hunting suppression, TCM simulation under existing control structure and changed control structure, existing feedforward controller of which is replaced to proposed feedforward controller, are performed. Both the original feedforward control and proposed one are applied to the 5th stand to directly compare the results. Exit thickness of the 5th stand, which is actually thickness of cold-rolled steel, is shown in Fig. 8 where the result of default control structure, control setting with proposed feedforward control, and desired thickness are expressed in blue dashed line, red line, and black thin dashed line, respectively. The RMSE of the 5th exit thickness for each case are given as table 5. Note that our proposed feedforward controller with hardness estimator significantly suppresses thickness hunting so that RMSE of the 5th exit thickness is reduced by 37% of default control structure. Here, the RMSE is calculated from normalized error to keep data security.

Table 5. RMSE of the 5th exit thickness

Controller	Original	Proposed
RMSE (%)	0.525	0.331

Not only the RMSE of 5th exit thickness but also off gauge length, which is the strip length violating given thickness error tolerance, can be used for the evaluation. The off gauge length for original/proposed feedforward control for three cases of error tolerances are given as table 6. Note that the off gauge length is directly connected to the profit, which means our proposed estimation framework and controller can significantly reduce the loss from the thickness hunting.

Table 6. Off gauge length for error tolerances

Tolerance (%)	Original	Proposed
± 2	22.13	6.98
± 2.5	8.69	5.25
± 3	6.39	0.00

5. CONCLUSION

We propose a novel hardness estimation framework for TCM (tandem col milling) process, which optimally fuses the nonlinear process model and available sensor information from each rolling stand, while also fully respecting the sparsity/scarcity of the sensors and the interconnected structure of the TCM process. We also devise a feedforward thickness hunting suppression control, which, by exploiting the estimated hardness information, can substantially reduce the thickness hunting of the TCM process. The proposed hardness estimation and feedforward control frameworks are then validated/verified with high-precision physics-based simulator of the TCM process.

REFERENCES

Bland, D. and Ford, H. (1943). The calculation of roll force and torque in cold strip rolling with tensions.

Proceedings of the Institution of Mechanical Engineers, 159(1), 144–163.

Bland, D., Ford, H., and Ellis, F. (1952). Cold rolling with strip tension. *Journal of Iron and Steel Institute*, 171(1), 245–249.

Bryant, G. (1973). *Automation of Tandem Mills*. British Iron and Steel Institute, London.

Bu, H., Yan, Z., and Zhang, D. (2019). A novel approach to improve the computing accuracy of rolling force and forward slip. *Ironmaking & Steelmaking*, 46(3), 269–276.

Choi, S., Johnson, M., and Grimble, M. (1994). Polynomial lqg control of back-up-roll eccentricity gauge variations in cold rolling mills. *Automatica*, 30(6), 975–992.

Geddes, E. and Postlethwaite, I. (1998). Improvements in product quality in tandem cold rolling using robust multivariable control. *IEEE transactions on control systems technology*, 6(2), 257–269.

Ha, C., Yoon, J., Kim, C., Lee, Y., Kwon, S., and Lee, D. (2018). Teleoperation of a platoon of distributed wheeled mobile robots with predictive display. *Autonomous Robots*, 42(8), 1819–1836.

Jazwinski, A. (2007). *Stochastic processes and filtering theory*. Courier Corporation.

Julier, S. (2002). The scaled unscented transformation. *In Proceedings of the 2002 American Control Conference (IEEE Cat. No. CH37301)*, 6, 4555–4559.

Orowan, E. (1943). The calculation of roll pressure in hot and cold flat rolling. *Proceedings of the Institution of Mechanical Engineers*, 150(1), 140–167.

Pittner, J. and Simaan, M. (2006). State-dependent ricaati equation approach for optimal control of a tandem cold metal rolling process. *IEEE transactions on industry applications*, 42(3), 836–843.

Pittner, J. and Simaan, M. (2008). Optimal control of tandem cold rolling using a pointwise linear quadratic technique with trims. *Journal of Dynamic Systems*, 130(2), 021006.

Prinz, K., Steinboeck, A., Mller, M., Ettl, A., Schausberger, F., and Kugi, A. (2019). Online parameter estimation for adaptive feedforward control of the strip thickness in a hot strip rolling mill. *Journal of Manufacturing Science and Engineering*, 141(7), 071005.

Roberts, W. (1978). *Cold rolling of steel*. Dekker.

Wang, J., Jiang, Z., Tieu, A., Liu, X., and Wang, G. (2005). Adaptive calculation of deformation resistance model of online process control in tandem cold mill. *Journal of Materials Processing Technology*, 162, 585–590.

Winkler, R. (1981). Combining probability distributions from dependent information sources. *Management Science*, 27(4), 479–488.